A&A 566, A104 (2014)
DOI: 10.1051/0004-6361/201423864
© ESO 2014

Astronomy & Astrophysics

# *R*-matrix electron-impact excitation data for the Be-like iso-electronic sequence⋆

L. Fernández-Menchero[1], G. Del Zanna[2], and N. R. Badnell[1]

[1] Department of Physics, University of Strathclyde, Glasgow G4 0NG, UK
e-mail: luis.fernandez-menchero@strath.ac.uk
[2] Department of Applied Mathematics and Theoretical Physics, University of Cambridge, Cambridge CB3 0WA, UK

Received 21 March 2014 / Accepted 15 May 2014

**ABSTRACT**

*Aims.* Emission lines from ions in the Be-like isoelectronic sequence can be used for reliable diagnostics of temperature and density of astrophysical and fusion plasmas over a wide range of temperatures. Surprisingly, interpolated data is all that is available for a number of astrophysically important ions.
*Methods.* We have carried out intermediate coupling frame transformation *R*-matrix calculations which include a total of 238 fine-structure levels in both the configuration interaction target and close-coupling collision expansions. These arise from the configurations $1s^2\,2\{s,p\}\,nl$ with $n = 3$–7, and $l = 0$–4 for $n \leq 5$ and $l = 0$–2 for $n = 6, 7$.
*Results.* We obtain ordinary collision strengths and Maxwell-averaged effective collision strengths for the electron-impact excitation of all the ions of the Be-like sequence, from $B^+$ to $Zn^{26+}$. We compare with previous *R*-matrix calculations and interpolated values for some benchmark ions. We find good agreement for transitions $n = 2$–2 with previous *R*-matrix calculations but some disagreements with interpolated values. We also find good agreement for the most intense transitions $n = 2$–3 which contribute via cascade to the ($n = 2$) diagnostic radiating levels.

**Key words.** atomic data – techniques: spectroscopic

## 1. Introduction

Emission lines from beryllium-like ions are used in astrophysics to study a variety of emission sources. For example, solar corona ultraviolet spectra (Vernazza & Reeves 1978; Sandlin et al. 1986) or solar flares (Neupert et al. 1967). Emission lines have been recorded by several solar missions, such as Skylab (Dere 1978). In the recent years, high-resolution XUV spectroscopic observations by *Chandra* and *XMM-Newton* satellites, have also shown that a vast number of astrophysical sources produce emission lines from Be-like ions, such as Fe XXIII (Audard 2003).

Many emission lines from Be-like ions have temperature or density sensitivity, so they can be used for diagnostics of astrophysical plasmas. In particular, the intensity ratios of the resonance versus the intercombination transitions in the Be-like ions is an excellent temperature diagnostic. The ratio between the $2s\,2p\,{}^1P_1$–$2p^2\,{}^1D_2$ and the intercombination transition is also a good diagnostic, considering that the lines always fall close in wavelength. Indeed, this ratio has provided one of very few direct measurements of electron temperatures in the solar corona from SOHO (see, e.g., Wilhelm et al. 1998). Be-like ion emission lines can be also used for diagnostics of fusion plasmas (Inoue et al. 2001; Summers et al. 1992).

Despite their importance, accurate electron impact excitation data for ions in this sequence are sparse. Coulomb-Born-plus-Exchange intermediate coupling (IC) calculations to $n = 3$ were carried out by Sampson et al. (1984) for seventeen ions between $Ne^{6+}$ and $W^{70+}$. *R*-matrix calculations were carried out by Berrington et al. (1985) for $C^{2+}$, $O^{4+}$, $Ne^{6+}$, and $Si^{10+}$ in *LS*-coupling followed by algebraic recoupling of the reactance matrices, only for transitions among the $n = 2$ levels (which give rise to ten fine-structure levels). The effective collision strengths of Berrington et al. (1985) were interpolated by Keenan et al. (1986) to provide data for $N^{3+}$, $F^{5+}$, $Na^{7+}$, $Mg^{8+}$, and $Al^{9+}$. With the addition of data for $Ca^{16+}$ from *R*-matrix calculations similar to Berrington et al. (1985) by Dufton et al. (1983), Keenan (1988) provided interpolated data for $P^{11+}$, $S^{12+}$, $Cl^{13+}$, $Ar^{14+}$, and $K^{15+}$. These two sets of interpolated rates have been widely used in the literature, and have been included in early versions of the CHIANTI database (Dere et al. 1997).

However, the irregular contribution of resonances to effective collision strengths along an iso-electronic sequence (Witthoeft et al. 2007) places an unknown uncertainty on such interpolated data. For example, significant problems with the interpolated values were found by Del Zanna et al. (2008). Del Zanna et al. (2008) performed an explicit *R*-matrix calculation for $Mg^{8+}$ and compared the intensities of the main lines with those obtained with the interpolated values. Significant differences (up to 50%) were found. There is therefore a need for explicit *R*-matrix calculations for all Be-like ions of astrophysical interest. This is the aim of the present work, which is part of a larger program of work to use the *R*-matrix method to calculate effective collision strengths for all ions, up to Zn, of all L-shell sequences as well as a start on the M-shell. The most recent sequence to-date is the B-like by Liang et al. (2012) and which contains references to earlier work on other sequences.

Some further *LS*-plus-algebraic recoupling *R*-matrix calculations were carried out by Ramsbottom and co-workers up to 2s3d (12 terms) for $N^{3+}$ (Ramsbottom et al. 1994b) and

⋆ These data are made available in the archives of APAP via http://www.apap-network.org and OPEN-ADAS via http://open.adas.ac.uk

up to 2p3d (26 terms) for $Ne^{6+}$ (Ramsbottom et al. 1994a; Ramsbottom et al. 1995). Zhang & Sampson (1992) obtained fully-relativistic distorted wave collision strengths, for transitions within the $n = 2$ complex, for all of the Be-like ions from $O^{4+}$ to $U^{88+}$. More recent fully-relativistic work includes distorted wave data (up to 2p4d and 2s5d) for $Si^{10+}$ by Bhatia & Landi (2007) and $R$-matrix results (up to $n = 5$) for $S^{12+}$, obtained using the Dirac $R$-matrix code (DARC) by Li et al. (2013).

Because of their importance to astrophysics, extensive IC $R$-matrix calculations for Be-like iron and nickel were carried out by Chidichimo et al. (2005; 2003) within the Iron Project, following an early distorted wave study by Bhatia & Mason (1981). In Chidichimo et al. (2005), collision strengths and effective collision strength were obtained for Be-like Fe for the configurations $n = 2, 3, 4$, including a total of 98 fine-structure levels in the basis set. A quite fine mesh was used for the electron impact energies, so the resonances were well resolved. In Del Zanna & Mason (2005), these atomic data were benchmarked against observations, pointing out temperature and density diagnostics. Overall good agreement between predicted and observed intensities was found. We therefore adopt this work on $Fe^{22+}$ as a benchmark of the whole sequence.

We also adopt the Del Zanna et al. (2008) results for $Mg^{8+}$ as a benchmark. Del Zanna et al. (2008) adopted the same target as Chidichimo et al. (2005) to calculate the scattering data for $Mg^{8+}$. They also benchmarked the atomic data against SOHO spectroscopic observations of the solar corona, finding excellent agreement, thus resolving long-standing discrepancies between observed and predicted line intensities. The use of $R$-matrix data resulted in significantly higher electron temperatures.

Finally, we also adopt as a benchmark the $R$-matrix results for $C^{2+}$ by Berrington et al. (1985, $n = 2$) and Berrington et al. (1989, $n = 3$). In this latter case ($n = 3$) no algebraic recoupling of the $LS$-coupling reactance matrices was carried out. Rather, when these data were uploaded to the CHIANTI database, level resolved data were obtained by splitting the $LS$-coupling effective collision strengths according to statistical weights (see Dere et al. 1997).

We note also that Mitnik et al. (2003) carried out an $R$-matrix with pseudostates calculation for $C^{2+}$, but only in $LS$-coupling. They found that inclusion of pseudostates reduced effective collision strengths for transitions $n = 2$–$3$ by typically 10% and those $n = 2$–$4$ by 20–30%. Furthermore, a similar $R$-matrix with pseudostates calculation by Badnell et al. (2003) found reductions of up to a factor of two in effective collision strengths for transitions to $n = 4$ in $B^+$. The effect of coupling to the continuum diminishes rapidly with increasing charge state though and so we would expect only modest overestimates for our $N^{3+}$ data.

In the present work we include states up to $n = 7$ in our configuration interaction (CI) expansion, for a total of 238 fine-structure levels. This basis set includes more bound states than any other previous non-pseudostate work and so levels up to $n = 4$ are better represented. In addition, cascading effects following collisional excitation up to the $n = 7$ shell can be examined with this basis set expansion. We use the same basis set and methods for the whole isoelectronic sequence, from $B^+$ to $Zn^{26+}$. The present data therefore includes significantly more transitions than the previous published works for ions in the same sequence.

Traditionally, astrophysics interest stops at Zn– for example, the Chianti and Cloudy modeling packages span H – Zn. This is because elemental abundance, e.g., solar, drops by over an order of magnitude at the next element onwards. However, we continue on up to Kr for magnetic fusion application. There-on, relativistic effects may need to be included in the wave functions themselves, e.g., via use of the Dirac $R$-matrix code. We leave no gaps because of the difficulty of deeming a priori those elements which will never be of interest to astrophysics or, especially, magnetic fusion. Any such would be small in number and so their omission not represent any significant saving of effort.

The paper is organised as follows. In Sect. 2 we give details of our description of the atomic structure and in Sect. 3 that of the $R$-matrix calculation. In Sect. 4 we show some representative results and compare them with the previous data of other $R$-matrix calculations or interpolated values. In Sect. 5 the main conclusions are discussed. Atomic units are used unless otherwise is specified.

## 2. Structure

To obtain the wave functions of the isolated target we used the AUTOSTRUCTURE program (Badnell 2011). AUTOSTRUCTURE calculates the wave functions by diagonalizing the Breit-Pauli Hamiltonian (Eissner et al. 1974), which includes the relativistic terms, mass-velocity, spin-orbit, and Darwin, as a perturbation. The electronic potential is included in terms of the Thomas-Fermi-Dirac-Amaldi model, adjusting the scaling parameters $\lambda$ through a variational method, minimizing the equally-weighted sum of all $LS$ term energies. We included a total of 21 atomic orbitals in the basis set: 1s, 2s, 2p, 3s, 3p, 3d, 4s, 4p, 4d, 4f, 5s, 5p, 5d, 5f, 5g, 6s, 6p, 6d, 7s, 7p, 7d. In the configuration interaction we included all the configurations $1s^2\,2s^2$, $1s^2\,2s\,2p$, $1s^2\,2p^2$, $1s^2\,2s\,nl$ and $1s^2\,2p\,nl$, with $nl$ all the orbitals previously mentioned with $n \geq 3$, for a total of 39 configurations. The minimized values of the scaling parameters are shown in Table 3 for all the ions in the sequence. As the atomic number increases, $\lambda$ for the 1s orbital increases far away from unity. This is due to the Darwin term becoming more important as the charge of the nucleus increases. This does not affect the actual atomic structure nor the values of the level energies. The values of $\lambda$ for orbitals with high angular momentum d, f and g are also much larger than the unity, which is necessary to influence the wave function for these eccentric orbits.

For such a configuration list we get a total of 130 $LS$ terms, which are split into 238 IC levels. The calculated target energies for the IC levels up to $n = 4$ of the sample ions $C^{2+}$, $Mg^{8+}$, and $Fe^{22+}$ are shown in Tables 4–6, respectively. They are compared with the observed ones, taken from the National Institute of Standards and Technology (NIST[1]) database (Moore 1993 for carbon, Martin & Zalubas 1980 for magnesium and Sugar & Corliss 1985 for iron) and previous theoretical works collected in the CHIANTI database (Berrington et al. 1985 for carbon $n = 2$, Berrington et al. 1989 for carbon $n = 3$, Del Zanna et al. 2008 for magnesium and Chidichimo et al. 2005 for iron). With a few exceptions in the lower excited singlet levels, the agreement with the observed values is within 1.5%. The deviation of the calculated energies respect the observed values is smaller in present work than in previous ones, only in the case of carbon it is larger than Berrington et al. (1985, 1989), this is due to their use of pseudo-orbitals. We prefer to use a spectroscopic orbitals so as to avoid having to deal with pseudo-resonances. In any case, our philosophy is to use the same approach to the structure along the entire sequence. The energy values for the rest of the levels and the other ions of the sequence not shown in Tables 4–6, can be found online. As with the previous sequences that we have considered, we use the calculated energies in the $R$-matrix calculation.

[1] http://physics.nist.gov

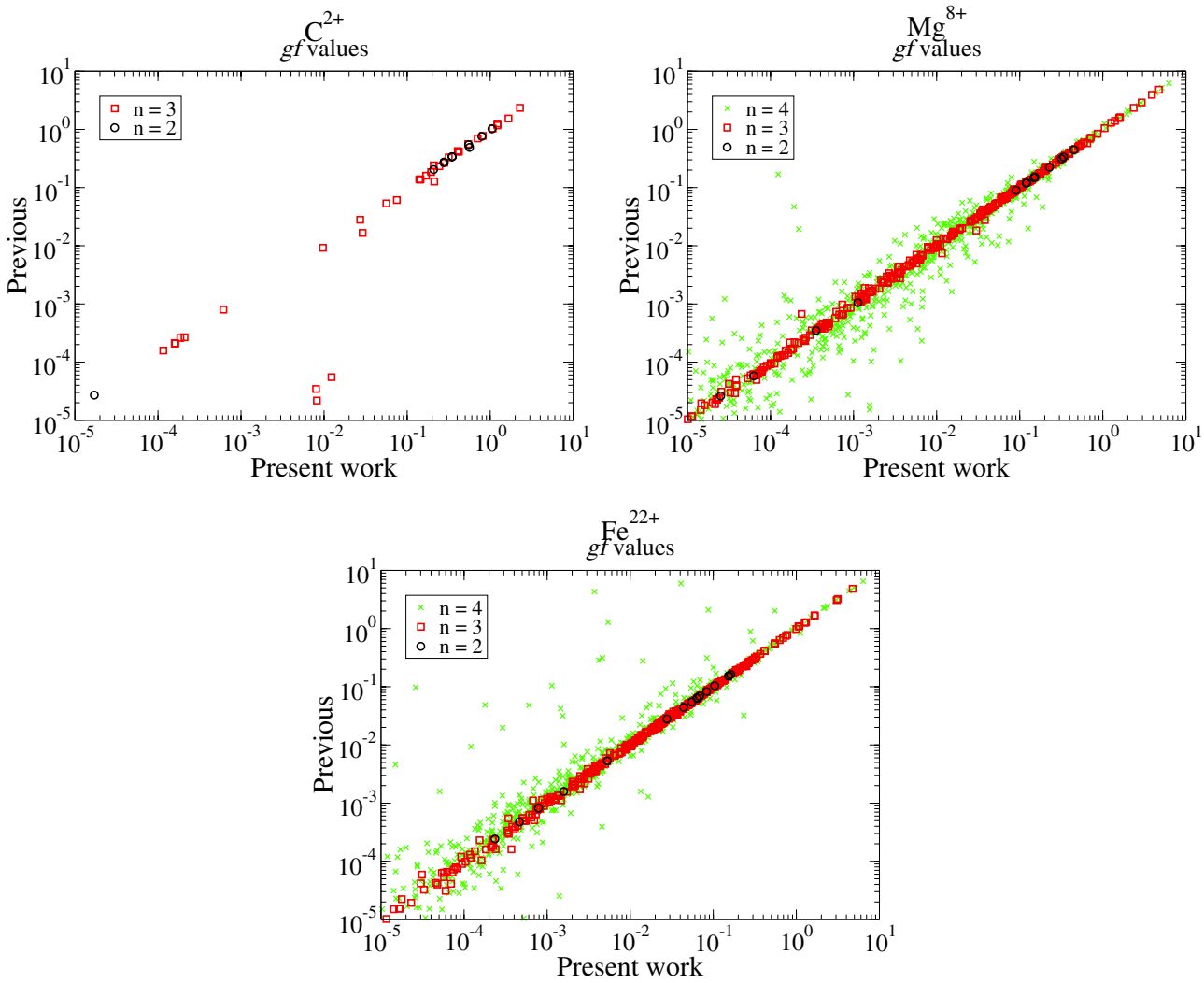


**Fig. 1.** Comparative plot of oscillator strengths for $C^{2+}$, $Mg^{8+}$, and $Fe^{22+}$. *x*-axis, present work; *y*-axis, refers to: $C^{2+}$ Tachiev & Fischer (1999), $Mg^{8+}$ Chidichimo et al. (2005), $Fe^{22+}$ Del Zanna et al. (2008); ∘ for $n = 2$ upper levels; □ for $n = 3$ upper levels; × for $n = 4$ upper levels.

**Table 1.** Comparison of $gf$ values for some selected transitions of the ion $Fe^{22+}$.

| Transition | $gf$ Present work | $gf$ C05 |
|---|---|---|
| 1 – 5 | 1.554 (−1) | 1.543 (−1) |
| 1 – 14 | 2.593 (−1) | 2.542 (−1) |
| 1 – 15 | 4.142 (−1) | 4.146 (−1) |
| 1 – 22 | 1.254 (−2) | 1.269 (−2) |
| 1 – 25 | 2.096 (−2) | 2.112 (−2) |
| 1 – 36 | 5.667 (−3) | 5.916 (−3) |
| 1 – 42 | 2.237 (−4) | 2.323 (−4) |
| 1 – 46 | 1.815 (−2) | 1.903 (−2) |
| 1 – 50 | 3.348 (−2) | 2.644 (−2) |
| 1 – 52 | 1.435 (−1) | 1.439 (−1) |
| 1 – 62 | 1.896 (−4) | 3.203 (−4) |
| 1 – 70 | 2.578 (−3) | 2.453 (−3) |

**Notes.** C05: Chidichimo et al. (2005). $A\,(B)$ denotes $A \times 10^B$.

To check the quality of the calculated wave functions of the target we compare the oscillator strengths ($gf$ values) for selected transitions in Table 1 for $Fe^{22+}$ with data from Chidichimo et al. (2005), which can be found on line in the CHIANTI database. Very good agreement is found, with the exception of the very weak transition 1−62: $2s^2\ ^1S_0$−$2p\,4s\ ^3P_1$.

Figure 1 shows a global comparison of oscillator strengths $gf$ for all the transitions between the levels shown in Tables 4–6, with the upper level with a configuration $2l\,nl'$ with $n \leq 4$, for the benchmark ions. We plot in the *x*-axis the present results, and in the *y*-axis the results of Tachiev & Fischer (1999) for carbon, Del Zanna et al. (2008) for magnesium, and Chidichimo et al. (2005) for iron. We note that the CHIANTI data for magnesium and iron are actually the results of separate structure calculations, and not those employed for the scattering target.

Points lying on the diagonal $x = y$ in Fig. 1 mean a full agreement between our calculation and previous ones. On the graph we display about 1200 $gf$ values and more than a 90% of them deviate less than a 5% from the diagonal. In carbon we appreciate four points far from the diagonal, they correspond to the transitions $2s^2\ ^1S_0$−$2s\,3p\ ^3P_1$, $2p^2\ ^1D_2$−$2s\,3p\ ^3P_1$, $2s\,3s\ ^1S_0$−$2s\,3p\ ^3P_1$ and $2p^2\ ^1S_0$−$2s\,3p\ ^3P_1$ (off the scale of the graph). Tachiev & Fischer (1999) used a multiconfiguration Hartree-Fock (MCHF) calculation followed by a configuration interaction (CI) calculation using the Breit-Pauli Hamiltonian. These transitions are forbidden ones as they are spin-changing, and the non-zero value of $gf$ comes from state mixing, between

the $^3P_1$ and the $^1P_1$. Such E1-transitions are very sensitive to the precise mixing. In carbon the nuclear charge is quite low, so the relativistic effects which can mix singlets and triplets are quite small. Repeating the AUTOSTRUCTURE calculation with different scaling parameters $\lambda$, we checked that the value of the $gf$ for those transitions is very sensitive and it can vary up to six orders of magnitude, nevertheless, the values of the level energies remain stable.

Such extreme sensitivity has little physical consequence. The radiative lifetime of the $2s\,3p\,^3P_1$ is dominated the strong E1-transition to $2s\,3s\,^3S_1$. The corresponding electron-impact excitation transitions are mediated by the two-body electrostatic exchange operator. As such, the effective collision strengths will behave for the most of the temperature range of interest as a forbiden transition, tending to zero. Only at high temperatures, above $10^6$ K, will a dipole tail appear tending to a non zero value. Such temperatures are much above the ionization temperature of $C^{2+}$. This sensitivity in such transition probabilities will also be reduced as the charge of the nucleus increases because the relativistic effects become larger and the state mixing fractions become more stable.

For iron and magnesium the agreement shown in Fig. 1 is very good, all the points for $n = 2, 3$ lie on the diagonal (less than a 5% of deviation) and about 90% of the $n = 4$ too, only the ones which correspond to weak transitions have a larger deviation. The points which lie far from the diagonal correspond to transitions between levels with configurations 4d and 4f, the last orbitals included in the basis sets of Chidichimo et al. (2005) and Del Zanna et al. (2008). As our basis set includes more bound orbitals, up to 7d, the description of these excited levels can vary respect the previous works and that is the likely reason for the discrepancy in the $gf$ values for those transitions.

## 3. Scattering

We use the $R$-matrix method (Hummer et al. 1993; Berrington et al. 1995) in combination with an intermediate coupling frame transformation (ICFT; Griffin et al. 1998; Badnell & Griffin 1999). The approach used is the same one as Chidichimo et al. (2005) and Del Zanna et al. (2008) for Be-like Fe and Mg, but with a larger close-coupling expansion.

In the $R$-matrix inner region, exchange effects were included for angular momentum up to $2J = 23$, then extended using a non-exchange approximation for $2J$ up to 89, the contributions for higher $J$ values were added using a top-up with the Burgess sum rule (Burgess 1974) for dipole transitions and a geometric series for the non-dipole transitions (Badnell & Griffin 2001). In the outer region we used two different meshes for the impact energy. A coarse mesh was applied for the non exchange calculation in the whole energy range and also for the exchange calculation for impact energies above the highest target level energy. This coarse mesh was around $10^{-4}z^2$ Ry, with $z$ the ion charge $Z - 4$, being $Z$ the atomic number.

The characteristic scattering energy increases as a factor $z^2$ with the charge of the ion, nevertheless the width of the resonances remains constant. In order to maintain the resolution of the resonances over the sequence, we should use a constant fine energy step, thus increasing the number of grid points by a factor $z^2$. This is computationally impractical for all but small calculations. In practice, we have found (Witthoeft et al. 2007) that increasing the number of grid points by a factor $z$ samples and converges the resonance structure satisfactorily. Thus, we use a fine energy mesh step which varies continuously versus the ionic charge, from $6.4 \times 10^{-5}$ for $B^+$ up to $2.2 \times 10^{-6}$ for $Zn^{26+}$.

**Table 2.** Comparison of (scaled) infinite energy limit points for some dipole (4S/3) and allowed (Born) transitions in $Fe^{22+}$.

| Transition | Ω Present work | Ω Previous |
|---|---|---|
| 1–12 | 1.732 (−2) | 1.640 (−2) |
| 1–18 | 2.296 (−4) | 2.115 (−4) |
| 1–20 | 4.785 (−2) | 4.784 (−2) |
| 1–26 | 7.889 (−5) | 9.233 (−5) |
| 1–28 | 6.840 (−6) | 5.990 (−6) |
| 1–32 | 2.725 (−5) | 2.413 (−5) |
| 1–35 | 9.170 (−5) | 1.099 (−4) |
| 1–37 | 1.763 (−4) | 2.369 (−4) |
| 1–40 | 9.745 (−6) | 8.954 (−6) |
| 1–44 | 4.097 (−5) | 3.779 (−5) |
| 1–45 | 1.594 (−4) | 1.548 (−4) |
| 1–48 | 3.478 (−3) | 2.995 (−3) |
| 1–54 | 6.394 (−5) | 6.059 (−5) |
| 1–56 | 7.296 (−3) | 7.435 (−3) |
| 1–58 | 9.053 (−5) | 7.548 (−5) |
| 1–60 | 2.611 (−3) | 2.573 (−3) |
| 1–65 | 3.928 (−6) | 4.455 (−6) |
| 1–66 | 1.528 (−5) | 1.050 (−5) |
| 1–69 | 1.036 (−5) | 8.712 (−6) |
| 1–73 | 4.017 (−5) | 3.922 (−5) |
| 1–75 | 5.630 (−6) | 5.013 (−6) |
| 1–78 | 2.107 (−6) | 2.314 (−6) |
| 1–79 | 5.146 (−6) | 6.350 (−6) |
| 1–84 | 1.638 (−6) | 1.230 (−6) |
| 1–85 | 4.304 (−5) | 2.907 (−5) |
| 1–90 | 1.757 (−7) | 1.864 (−7) |
| 1–91 | 1.356 (−5) | 4.049 (−5) |
| 1–94 | 8.444 (−6) | 7.422 (−6) |
| 1–95 | 2.408 (−5) | 1.964 (−5) |
| 1–98 | 4.034 (−5) | 1.338 (−5) |

**Notes.** Previous: Chidichimo et al. (2005). $A\,(B)$ denotes $A \times 10^B$.

We convoluted the collision strengths $\Omega(i - j)$ with a Maxwellian distribution for the energies of the plasma electrons to form integrated effective collision strengths $\Upsilon(i - j)$:

$$\Upsilon(i - j) = \int_0^\infty \mathrm{d}u\, \mathrm{e}^{-u}\, \Omega(i - j), \quad (1)$$

where $u = E/kT$ and $E$ is the energy of the scattered electron, $T$ the electron temperature and $k$ the Boltzmann constant. We calculated the effective collision strengths for a wide range of temperatures from $1.6 \times 10^4$ to $1.6 \times 10^8$ K, which covers the whole range of interest for astrophysical and fusion plasmas.

For this integration, the collision strengths were extended to high energies by interpolation using the appropriate infinite-energy limits in the Burgess & Tully (1992) scaled domain. The infinite-energy limits were calculated with AUTOSTRUCTURE depending on the transition type: for the dipole-allowed transitions the results are given by $4S/3$, where $S$ is the line strength, and for the non-dipole-allowed transitions by the Born approximation as described in Burgess et al. (1997). This infinite energy point can also be used to compare the present atomic structure with the previous ones. In Table 2 we show a comparison between the values of the collision strengths for infinite impact energy with the ones calculated by Chidichimo et al. (2005). Agreement below the 5% is found in most cases, with larger discrepancies present for the higher $n = 4$ levels.

**Table 3.** Thomas-Fermi-Dirac-Amaldi potential scaling factors used in AUTOSTRUCTURE calculation.

| Ion | 1s | 2s | 2p | 3s | 3p | 3d | 4s | 4p | 4d | 4f | |
|---|---|---|---|---|---|---|---|---|---|---|---|
| | 5s | 5p | 5d | 5f | 5g | 6s | 6p | 6d | 7s | 7p | 7d |
| $B^{+}$ | 1.39653 | 1.46875 | 1.43661 | 1.19439 | 1.14553 | 1.29613 | 1.19203 | 1.13186 | 1.29804 | 1.45128 | |
| | 1.19330 | 1.12751 | 1.30168 | 1.45196 | 1.57425 | 1.19540 | 1.12564 | 1.30678 | 1.19849 | 1.12477 | 1.31345 |
| $C^{2+}$ | 1.41290 | 1.49099 | 1.43422 | 1.20193 | 1.13345 | 1.27955 | 1.20122 | 1.12308 | 1.28131 | 1.43825 | |
| | 1.20319 | 1.11983 | 1.28608 | 1.44185 | 1.57035 | 1.20542 | 1.11806 | 1.29188 | 1.20938 | 1.11667 | 1.29554 |
| $N^{3+}$ | 1.43000 | 1.50845 | 1.43689 | 1.21092 | 1.13140 | 1.27332 | 1.21098 | 1.12277 | 1.27607 | 1.43341 | |
| | 1.21343 | 1.12037 | 1.28215 | 1.43924 | 1.55457 | 1.21659 | 1.11834 | 1.28456 | 1.22184 | 1.11739 | 1.28733 |
| $O^{4+}$ | 1.44986 | 1.52368 | 1.44080 | 1.22007 | 1.13315 | 1.27102 | 1.22074 | 1.12656 | 1.27530 | 1.44272 | |
| | 1.22378 | 1.12262 | 1.27931 | 1.44190 | 1.54473 | 1.22792 | 1.12112 | 1.28112 | 1.23339 | 1.11910 | 1.28155 |
| $F^{5+}$ | 1.47345 | 1.53823 | 1.44532 | 1.23007 | 1.13634 | 1.27176 | 1.23140 | 1.12941 | 1.27676 | 1.45042 | |
| | 1.23579 | 1.12547 | 1.27851 | 1.44190 | 1.58397 | 1.23970 | 1.12653 | 1.27874 | 1.24668 | 1.12543 | 1.27878 |
| $Ne^{6+}$ | 1.50238 | 1.61111 | 1.44991 | 1.24485 | 1.13968 | 1.27306 | 1.24651 | 1.13170 | 1.27109 | 1.45896 | |
| | 1.25340 | 1.12866 | 1.27787 | 1.46014 | 0.17214 | 1.25114 | 1.12823 | 1.27534 | 1.25978 | 1.13215 | 1.29033 |
| $Na^{7+}$ | 1.53841 | 1.56981 | 1.45496 | 1.25454 | 1.14548 | 1.27582 | 1.25766 | 1.14271 | 1.27844 | 1.45585 | |
| | 1.25613 | 1.13208 | 1.27826 | 1.49334 | 1.69385 | 1.26776 | 1.16973 | 1.28085 | 1.28134 | 1.13540 | 1.30630 |
| $Mg^{8+}$ | 1.24000 | 1.59549 | 1.46744 | 1.27389 | 1.15697 | 1.27971 | 1.27754 | 1.15316 | 1.28140 | 2.06981 | |
| | 1.28021 | 1.14906 | 1.27926 | 1.50322 | 1.89909 | 1.28950 | 1.14724 | 1.29386 | 1.28025 | 1.15310 | 1.31404 |
| $Al^{9+}$ | 1.25000 | 1.61669 | 1.47329 | 1.29225 | 1.16420 | 1.28342 | 1.29693 | 1.16044 | 1.28450 | 1.96809 | |
| | 1.29904 | 1.17984 | 1.28149 | 1.52430 | 1.85742 | 1.30930 | 1.15922 | 1.30526 | 1.30787 | 1.16520 | 1.32541 |
| $Si^{10+}$ | 1.27000 | 1.63993 | 1.48096 | 1.31345 | 1.17269 | 1.28795 | 1.31899 | 1.16446 | 1.28771 | 1.50502 | |
| | 1.32219 | 1.16996 | 1.29524 | 1.52410 | 1.86078 | 1.33213 | 1.17292 | 1.31636 | 1.33749 | 1.17722 | 1.33820 |
| $P^{11+}$ | 1.29000 | 1.66698 | 1.48863 | 1.33792 | 1.18239 | 1.29330 | 1.34453 | 1.17405 | 1.29175 | 1.52229 | |
| | 1.32916 | 1.17753 | 1.30630 | 1.54557 | 1.86065 | 1.36058 | 1.17768 | 1.32799 | 1.35421 | 1.18970 | 1.34597 |
| $S^{12+}$ | 1.32000 | 1.69798 | 1.49820 | 1.36619 | 1.19385 | 1.29928 | 1.37362 | 1.18607 | 1.29705 | 1.54291 | |
| | 1.37509 | 1.18607 | 1.31273 | 1.54252 | 1.85894 | 1.40135 | 1.19959 | 1.36643 | 1.38328 | 1.20349 | 1.35765 |
| $Cl^{13+}$ | 1.34000 | 1.73414 | 1.51315 | 1.39842 | 1.20570 | 1.30618 | 1.40687 | 1.41009 | 1.30748 | 1.56630 | |
| | 1.44054 | 1.20384 | 1.33685 | 1.60963 | 1.85107 | 1.38976 | 1.21181 | 1.35402 | 1.41456 | 1.21988 | 1.36876 |
| $Ar^{14+}$ | 1.38000 | 1.77486 | 1.51919 | 1.43674 | 1.22246 | 1.31414 | 1.44543 | 1.21480 | 1.32216 | 1.57071 | |
| | 1.44720 | 1.21869 | 1.36034 | 1.59897 | 1.77197 | 1.42508 | 1.22830 | 1.36468 | 1.45103 | 1.23554 | 1.38174 |
| $K^{15+}$ | 1.42000 | 1.82173 | 1.53065 | 1.47991 | 1.23087 | 1.32155 | 1.48906 | 1.23105 | 1.33713 | 1.59368 | |
| | 1.48858 | 1.24032 | 1.38104 | 1.62515 | 2.10990 | 1.48167 | 1.24772 | 1.37835 | 1.49367 | 1.25383 | 1.39537 |
| $Ca^{16+}$ | 1.47000 | 1.87511 | 1.54387 | 1.52883 | 1.24783 | 1.32959 | 1.53787 | 1.25088 | 1.35215 | 1.61528 | |
| | 1.53483 | 1.26078 | 1.37265 | 1.65110 | 2.12513 | 1.53123 | 1.26716 | 1.39392 | 1.54165 | 1.27363 | 1.41068 |
| $Sc^{17+}$ | 1.53000 | 1.93788 | 1.59589 | 1.75156 | 1.26621 | 1.33795 | 1.59469 | 1.27257 | 1.36750 | 1.63587 | |
| | 1.58985 | 1.28349 | 1.39183 | 1.67574 | 2.15051 | 1.58759 | 1.29120 | 1.40896 | 1.59725 | 1.29707 | 1.42576 |
| $Ti^{18+}$ | 1.60000 | 2.00584 | 1.57603 | 1.65114 | 1.27591 | 1.35026 | 1.65665 | 1.29754 | 1.38595 | 1.65776 | |
| | 1.65154 | 1.30781 | 1.41023 | 1.70303 | 2.19714 | 1.65227 | 1.31642 | 1.42776 | 1.66059 | 1.32362 | 1.44441 |
| $V^{19+}$ | 1.68000 | 2.08529 | 1.59641 | 1.72470 | 1.36143 | 1.36267 | 1.72709 | 1.32503 | 1.40464 | 1.68328 | |
| | 1.72037 | 1.33534 | 1.42895 | 1.73176 | 2.23923 | 1.68904 | 1.34592 | 1.44648 | 1.73785 | 1.33680 | 1.46407 |
| $Cr^{20+}$ | 1.79000 | 2.17707 | 1.61657 | 1.80606 | 1.33031 | 1.37636 | 1.80500 | 1.35470 | 1.42787 | 1.70784 | |
| | 1.79735 | 1.36558 | 1.44939 | 1.76243 | 2.23933 | 1.77710 | 1.37646 | 1.46636 | 1.84642 | 1.37410 | 1.48713 |
| $Mn^{21+}$ | 1.92000 | 2.28271 | 1.63986 | 1.89840 | 1.35947 | 1.39912 | 1.90077 | 1.38817 | 1.43396 | 1.73446 | |
| | 1.88281 | 1.39830 | 1.47158 | 1.79320 | 2.30111 | 1.86717 | 1.39472 | 1.49170 | 1.77849 | 1.39979 | 1.50936 |
| $Fe^{22+}$ | 2.09000 | 2.40609 | 1.66339 | 2.00074 | 1.39088 | 1.41977 | 1.98780 | 1.42379 | 1.46599 | 1.76469 | |
| | 1.97794 | 1.43521 | 1.49892 | 1.82733 | 2.37774 | 1.96099 | 1.43770 | 1.51479 | 1.92026 | 1.44292 | 1.53397 |
| $Co^{23+}$ | 2.33000 | 2.55047 | 1.69200 | 2.11526 | 1.42494 | 1.44148 | 2.09657 | 1.46324 | 1.48980 | 1.79380 | |
| | 2.08337 | 1.47543 | 1.52191 | 1.86205 | 2.38007 | 2.06500 | 1.50871 | 1.54053 | 2.03551 | 1.51276 | 1.56093 |
| $Ni^{24+}$ | 2.66000 | 2.72055 | 1.72256 | 2.24298 | 1.46199 | 1.46465 | 2.21669 | 1.50708 | 1.51495 | 1.82611 | |
| | 2.20013 | 1.55010 | 1.54587 | 1.89817 | 2.45661 | 2.18012 | 1.55583 | 1.56840 | 2.15389 | 1.55986 | 1.58994 |
| $Cu^{25+}$ | 3.16000 | 2.92546 | 1.76525 | 2.38879 | 1.50301 | 1.48887 | 2.35148 | 1.55565 | 1.54173 | 1.85563 | |
| | 2.33131 | 1.59550 | 1.57404 | 1.93698 | 2.52032 | 2.30874 | 1.60920 | 1.59817 | 2.28313 | 1.61318 | 1.63090 |
| $Zn^{26+}$ | 4.03000 | 3.21931 | 1.79979 | 2.54953 | 1.54609 | 1.51586 | 2.49745 | 1.60297 | 1.57155 | 1.88843 | |
| | 2.48067 | 1.65834 | 1.60621 | 1.97794 | 2.58467 | 2.44457 | 1.66547 | 1.62761 | 2.41800 | 1.66841 | 1.65212 |

## 4. Results

We calculated the collision strengths $\Omega(i-j)$ and effective collision strengths $\Upsilon(i-j)$ for the electron impact excitation of ions in the Be-like isoelectronic sequence, from $B^{+}$ to $Zn^{26+}$, for all transitions between the first 238 fine structure levels. This results in a total of 28 203 transitions for each ion.

The effective collision strengths $\Upsilon(i-j)$ have been stored as an Atomic Data Format file *adf04*. These files also contain the full set of one-photon allowed transition $A$-values calculated with AUTOSTRUCTURE. These data can be used for diagnostic of temperature and density of astrophysical and fusion plasmas. Nevertheless, for non Maxwellian velocity distributions in plasma, these *adf04* files can not be used and the collision strengths $\Omega$ should be used directly.

As a sample of the results, we show in Fig. 2 the collision strengths for some important transitions within the $n = 2$ complex (see Del Zanna et al. 2008) for the benchmark ions in the

**Table 4.** $C^{2+}$ target levels.

| $i$ | Conf. | Level | $E_{th}$ ( %) | $E_{NIST}$ | $E_{CHIANTI}$ ( %) | $i$ | Conf. | Level | $E_{th}$ ( %) | $E_{NIST}$ | $E_{CHIANTI}$ (%) |
|---|---|---|---|---|---|---|---|---|---|---|---|
| 1 | $2s^2$ | $^1S_0$ | 0. ( −) | 0. | 0. ( −) | 50 | 2p 3d | $^3F^o_4$ | 332 279. (0.4) | 333 447. | − ( −) |
| 2 | 2s 2p | $^3P^o_0$ | 53 715. (2.6) | 52 367. | 52 432. (0.1) | 51 | 2p 3p | $^1D_2$ | 333 829. (0.2) | 333 118. | − ( −) |
| 3 | 2s 2p | $^3P^o_1$ | 53 750. (2.6) | 52 391. | 52 432. (0.1) | 52 | 2p 3d | $^3D^o_1$ | 335 540. (0.6) | 337 656. | − ( −) |
| 4 | 2s 2p | $^3P^o_2$ | 53 820. (2.6) | 52 447. | 52 432. (0.0) | 53 | 2p 3d | $^3D^o_2$ | 335 554. (0.6) | 337 669. | − ( −) |
| 5 | 2s 2p | $^1P^o_1$ | 110 046. (7.5) | 102 352. | 103 252. (0.9) | 54 | 2p 3d | $^3D^o_3$ | 335 575. (0.6) | 337 688. | − ( −) |
| 6 | $2p^2$ | $^3P_0$ | 141 612. (3.0) | 137 426. | 138 247. (0.6) | 55 | 2s 5s | $^1S_0$ | 335 888. (0.8) | 338 514. | − ( −) |
| 7 | $2p^2$ | $^3P_1$ | 141 646. (3.0) | 137 454. | 138 247. (0.6) | 56 | 2s 5s | $^3S_1$ | 336 531. (1.0) | 339 935. | − ( −) |
| 8 | $2p^2$ | $^3P_2$ | 141 715. (3.1) | 137 502. | 138 247. (0.5) | 57 | 2p 3d | $^3P^o_2$ | 337 994. (0.6) | 340 102. | − ( −) |
| 9 | $2p^2$ | $^1D_2$ | 154 426. (5.9) | 145 876. | 146 422. (0.4) | 58 | 2p 3d | $^3P^o_1$ | 338 014. (0.6) | 340 128. | − ( −) |
| 10 | $2p^2$ | $^1S_0$ | 194 713. (6.7) | 182 520. | 185 094. (1.4) | 59 | 2p 3d | $^3P^o_0$ | 338 024. (0.6) | 340 142. | − ( −) |
| 11 | 2s 3s | $^3S_1$ | 235 036. (1.3) | 238 213. | 237 164. (0.4) | 60 | 2s 5f | $^1F^o_3$ | 340 059. (2.5) | 348 860. | − ( −) |
| 12 | 2s 3s | $^1S_0$ | 244 899. (0.9) | 247 170. | 246 492. (0.3) | 61 | 2s 5p | $^1P^o_1$ | 340 665. (0.8) | 343 258. | − ( −) |
| 13 | 2s 3p | $^1P^o_1$ | 256 774. (0.8) | 258 931. | 258 223. (0.3) | 62 | 2s 5p | $^3P^o_2$ | 341 178. (0.9) | 344 233. | − ( −) |
| 14 | 2s 3p | $^3P^o_0$ | 256 810. (1.1) | 259 706. | 258 881. (0.3) | 63 | 2s 5p | $^3P^o_1$ | 341 187. (0.9) | 344 236. | − ( −) |
| 15 | 2s 3p | $^3P^o_1$ | 256 818. (1.1) | 259 711. | 258 881. (0.3) | 64 | 2s 5p | $^3P^o_0$ | 341 191. (0.9) | 344 239. | − ( −) |
| 16 | 2s 3p | $^3P^o_2$ | 256 829. (1.1) | 259 724. | 258 881. (0.3) | 65 | 2s 5d | $^3D_1$ | 342 134. (1.0) | 345 497. | − ( −) |
| 17 | 2s 3d | $^3D_1$ | 267 262. (1.0) | 270 011. | 268 922. (0.4) | 66 | 2s 5d | $^3D_2$ | 342 134. (1.0) | 345 497. | − ( −) |
| 18 | 2s 3d | $^3D_2$ | 267 264. (1.0) | 270 012. | 268 922. (0.4) | 67 | 2s 5d | $^3D_3$ | 342 135. (1.0) | 345 497. | − ( −) |
| 19 | 2s 3d | $^3D_3$ | 267 268. (1.0) | 270 015. | 268 922. (0.4) | 68 | 2s 5g | $^3G_3$ | 343 014. (1.0) | 346 579. | − ( −) |
| 20 | 2s 3d | $^1D_2$ | 275 338. (0.4) | 276 483. | 276 308. (0.1) | 69 | 2s 5g | $^3G_4$ | 343 015. (1.0) | 346 579. | − ( −) |
| 21 | 2s 4s | $^3S_1$ | 306 319. (1.0) | 309 457. | − ( −) | 70 | 2s 5g | $^3G_5$ | 343 015. (1.0) | 346 579. | − ( −) |
| 22 | 2p 3s | $^3P^o_0$ | 306 368. (0.6) | 308 217. | − ( −) | 71 | 2s 5g | $^1G_4$ | 343 015. (1.0) | 346 579. | − ( −) |
| 23 | 2p 3s | $^3P^o_1$ | 306 403. (0.6) | 308 249. | − ( −) | 72 | 2s 5d | $^1D_2$ | 343 749. (0.8) | 346 658. | − ( −) |
| 24 | 2p 3s | $^3P^o_2$ | 306 475. (0.6) | 308 317. | − ( −) | 73 | 2s 5f | $^3F^o_2$ | 343 914. (0.9) | 347 152. | − ( −) |
| 25 | 2p 3s | $^1P^o_1$ | 308 394. (0.5) | 310 006. | − ( −) | 74 | 2s 5f | $^3F^o_3$ | 343 916. (0.9) | 347 153. | − ( −) |
| 26 | 2s 4s | $^1S_0$ | 308 465. (1.0) | 311 722. | − ( −) | 75 | 2s 5f | $^3F^o_4$ | 343 920. (0.9) | 347 155. | − ( −) |
| 27 | 2s 4p | $^3P^o_0$ | 314 505. (1.0) | 317 794. | − ( −) | 76 | 2p 3p | $^1S_0$ | 346 252. (0.3) | 345 095. | − ( −) |
| 28 | 2s 4p | $^3P^o_1$ | 314 508. (1.0) | 317 797. | − ( −) | 77 | 2p 3d | $^1P^o_1$ | 346 391. (0.1) | 346 713. | − ( −) |
| 29 | 2s 4p | $^3P^o_2$ | 314 512. (1.0) | 317 801. | − ( −) | 78 | 2p 3d | $^1F^o_3$ | 348 219. (2.0) | 341 371. | − ( −) |
| 30 | 2p 3p | $^1P_1$ | 317 694. (0.6) | 319 720. | − ( −) | 79 | 2s 6s | $^3S_1$ | 351 405. (1.0) | 354 858. | − ( −) |
| 31 | 2s 4d | $^3D_1$ | 318 501. (0.9) | 321 411. | − ( −) | 80 | 2s 6s | $^1S_0$ | 352 937. ( −) | − | − ( −) |
| 32 | 2s 4d | $^3D_2$ | 318 507. (0.9) | 321 427. | − ( −) | 81 | 2s 6p | $^3P^o_0$ | 353 549. (1.0) | 357 049. | − ( −) |
| 33 | 2s 4d | $^3D_3$ | 318 517. (0.9) | 321 450. | − ( −) | 82 | 2s 6p | $^3P^o_1$ | 353 550. (1.0) | 357 050. | − ( −) |
| 34 | 2s 4f | $^3F^o_2$ | 318 840. (1.0) | 322 004. | − ( −) | 83 | 2s 6p | $^3P^o_2$ | 353 551. (1.0) | 357 051. | − ( −) |
| 35 | 2s 4f | $^3F^o_3$ | 318 846. (1.0) | 322 010. | − ( −) | 84 | 2s 6p | $^1P^o_1$ | 353 819. (0.9) | 357 110. | − ( −) |
| 36 | 2s 4f | $^3F^o_4$ | 318 853. (1.0) | 322 018. | − ( −) | 85 | 2s 6d | $^3D_1$ | 354 636. (1.0) | 358 098. | − ( −) |
| 37 | 2s 4f | $^1F^o_3$ | 319 376. (1.0) | 322 702. | − ( −) | 86 | 2s 6d | $^3D_2$ | 354 636. (1.0) | 358 098. | − ( −) |
| 38 | 2p 3p | $^3D_1$ | 321 171. (0.6) | 323 077. | − ( −) | 87 | 2s 6d | $^3D_3$ | 354 637. (1.0) | 358 098. | − ( −) |
| 39 | 2p 3p | $^3D_2$ | 321 206. (0.6) | 323 101. | − ( −) | 88 | 2s 6d | $^1D_2$ | 355 514. (0.9) | 358 733. | − ( −) |
| 40 | 2p 3p | $^3D_3$ | 321 260. (0.6) | 323 140. | − ( −) | 89 | 2s 7s | $^3S_1$ | 360 131. (1.0) | 363 613. | − ( −) |
| 41 | 2s 4d | $^1D_2$ | 321 734. (0.8) | 324 212. | − ( −) | 90 | 2s 7s | $^1S_0$ | 360 660. ( −) | − | − ( −) |
| 42 | 2s 4p | $^1P^o_1$ | 321 867. (0.2) | 322 404. | − ( −) | 91 | 2s 7p | $^3P^o_0$ | 361 434. ( −) | − | − ( −) |
| 43 | 2p 3p | $^3S_1$ | 325 461. (0.6) | 327 278. | − ( −) | 92 | 2s 7p | $^3P^o_1$ | 361 434. ( −) | − | − ( −) |
| 44 | 2p 3p | $^3P_0$ | 328 376. (0.4) | 329 685. | − ( −) | 93 | 2s 7p | $^3P^o_2$ | 361 435. ( −) | − | − ( −) |
| 45 | 2p 3p | $^3P_1$ | 328 399. (0.4) | 329 706. | − ( −) | 94 | 2s 7p | $^1P^o_1$ | 361 466. (0.9) | 364 896. | − ( −) |
| 46 | 2p 3p | $^3P_2$ | 328 442. (0.4) | 329 744. | − ( −) | 95 | 2s 7d | $^3D_1$ | 362 131. (1.0) | 365 638. | − ( −) |
| 47 | 2p 3d | $^1D^o_2$ | 330 524. (0.7) | 332 691. | − ( −) | 96 | 2s 7d | $^3D_2$ | 362 131. (1.0) | 365 638. | − ( −) |
| 48 | 2p 3d | $^3F^o_2$ | 332 208. (0.4) | 333 387. | − ( −) | 97 | 2s 7d | $^3D_3$ | 362 132. (1.0) | 365 638. | − ( −) |
| 49 | 2p 3d | $^3F^o_3$ | 332 238. (0.4) | 333 412. | − ( −) | 98 | 2s 7d | $^1D_2$ | 362 681. (0.9) | 366 028. | − ( −) |

**Notes.** Key: $i$: level index; Conf.: configuration; Level: level IC designation; $E_{th}$: theoretical level energy ($cm^{-1}$), this work; $E_{NIST}$: observed energy from the NIST database and reference Moore (1993) ($cm^{-1}$); $E_{CHIANTI}$: previous theoretical calculation of Berrington et al. (1985, 1989) as in the CHIANTI database; %: percentage difference between theoretical and NIST data.

Be-like sequence. We show four different types of transitions: dipole-allowed (1−5), dipole-allowed through spin-orbit mixing (1−3), a double-electron-jump Born transition (1−9), and a forbidden one (1−4). The collision strengths present the usual structure, a resonance region for the energies which correspond to transitions between the calculated levels, and a regular background. For dipole-allowed transitions, the collision strength diverges logarithmically as the energy tends to infinity, while for non dipole-allowed transitions it tends to a constant and for forbidden transitions the collision strength tends to zero as $E^{-2}$ in the infinite energy limit.

Looking down the columns of Fig. 2 we can follow the isoelectronic trend, or lack thereof, of a transition. The resonance structure and background varies differently as the ion charge increases. The resonance widths remain constant while the impact energy increases as a factor $z^2$. The height of the resonances

**Table 5.** $Mg^{8+}$ target levels.

| $i$ | Conf. | Level | $E_{th}$ ( %) | $E_{NIST}$ | $E_{CHIANTI}$ ( %) | $i$ | Conf. | Level | $E_{th}$ ( %) | $E_{NIST}$ | $E_{CHIANTI}$ ( %) |
|---|---|---|---|---|---|---|---|---|---|---|---|
| 1 | $2s^2$ | $^1S_0$ | 0. ( –) | 0. | 0. ( –) | 50 | 2s 4p | $^3P^o_1$ | 2 063 734. ( –) | – | 2 064 924. ( –) |
| 2 | 2s 2p | $^3P^o_0$ | 140 982. (0.3) | 140 504. | 141 277. (0.6) | 51 | 2s 4p | $^3P^o_2$ | 2 064 011. ( –) | – | 2 065 186. ( –) |
| 3 | 2s 2p | $^3P^o_1$ | 142 270. (0.5) | 141 631. | 142 555. (0.7) | 52 | 2s 4p | $^1P^o_1$ | 2 066 449. (0.1) | 2 068 680. | 2 067 943. (0.0) |
| 4 | 2s 2p | $^3P^o_2$ | 144 920. (0.6) | 144 091. | 145 184. (0.8) | 53 | 2s 4d | $^3D_1$ | 2 077 595. (0.1) | 2 079 970. | 2 078 838. (0.1) |
| 5 | 2s 2p | $^1P^o_1$ | 278 399. (2.5) | 271 687. | 279 967. (3.0) | 54 | 2s 4d | $^3D_2$ | 2 077 645. (0.1) | 2 079 970. | 2 078 885. (0.1) |
| 6 | $2p^2$ | $^3P_0$ | 369 168. (0.9) | 365 856. | 369 930. (1.1) | 55 | 2s 4d | $^3D_3$ | 2 077 720. (0.1) | 2 080 050. | 2 078 957. (0.1) |
| 7 | $2p^2$ | $^3P_1$ | 370 555. (0.9) | 367 159. | 371 306. (1.1) | 56 | 2s 4d | $^1D_2$ | 2 086 270. (0.1) | 2 087 890. | 2 087 551. (0.0) |
| 8 | $2p^2$ | $^3P_2$ | 373 076. (1.0) | 369 330. | 373 811. (1.2) | 57 | 2s 4f | $^3F^o_2$ | 2 086 530. ( –) | – | 2 087 845. ( –) |
| 9 | $2p^2$ | $^1D_2$ | 413 143. (2.0) | 405 100. | 414 538. (2.3) | 58 | 2s 4f | $^3F^o_3$ | 2 086 558. ( –) | – | 2 087 874. ( –) |
| 10 | $2p^2$ | $^1S_0$ | 513 046. (2.7) | 499 633. | 514 353. (2.9) | 59 | 2s 4f | $^3F^o_4$ | 2 086 597. ( –) | – | 2 087 912. ( –) |
| 11 | 2s 3s | $^3S_1$ | 1 529 401. (0.2) | 1 532 450. | 1 530 734. (0.1) | 60 | 2s 4f | $^1F^o_3$ | 2 089 095. ( –) | – | 2 090 438. ( –) |
| 12 | 2s 3s | $^1S_0$ | 1 555 861. (0.1) | 1 558 080. | 1 556 824. (0.1) | 61 | 2p 4s | $^3P^o_0$ | 2 205 006. ( –) | – | 2 206 147. ( –) |
| 13 | 2s 3p | $^1P^o_1$ | 1 591 800. (0.1) | 1 593 600. | 1 593 190. (0.0) | 62 | 2p 4s | $^3P^o_1$ | 2 205 866. ( –) | – | 2 207 065. ( –) |
| 14 | 2s 3p | $^3P^o_0$ | 1 594 402. (0.2) | 1 597 500. | 1 595 438. (0.1) | 63 | 2p 4s | $^3P^o_2$ | 2 208 975. ( –) | – | 2 210 045. ( –) |
| 15 | 2s 3p | $^3P^o_1$ | 1 594 786. (0.2) | 1 597 500. | 1 595 820. (0.1) | 64 | 2p 4s | $^1P^o_1$ | 2 213 758. ( –) | – | 2 216 284. ( –) |
| 16 | 2s 3p | $^3P^o_2$ | 1 595 382. (0.1) | 1 597 500. | 1 596 396. (0.1) | 65 | 2p 4p | $^1P_1$ | 2 222 434. ( –) | – | 2 223 811. ( –) |
| 17 | 2s 3d | $^3D_1$ | 1 629 120. (0.1) | 1 631 040. | 1 630 250. (0.0) | 66 | 2p 4p | $^3D_1$ | 2 225 037. (0.2) | 2 229 730. | 2 226 363. (0.2) |
| 18 | 2s 3d | $^3D_2$ | 1 629 265. (0.1) | 1 631 170. | 1 630 392. (0.0) | 67 | 2p 4p | $^3D_2$ | 2 225 527. (0.2) | 2 229 730. | 2 226 814. (0.1) |
| 19 | 2s 3d | $^3D_3$ | 1 629 481. (0.1) | 1 631 320. | 1 630 606. (0.0) | 68 | 2p 4p | $^3D_3$ | 2 228 012. (0.1) | 2 229 730. | 2 229 254. (0.0) |
| 20 | 2s 3d | $^1D_2$ | 1 655 247. (0.0) | 1 654 580. | 1 656 673. (0.1) | 69 | 2p 4p | $^3S_1$ | 2 229 779. ( –) | – | 2 232 150. ( –) |
| 21 | 2p 3s | $^3P^o_0$ | 1 708 717. (0.1) | 1 710 140. | 1 709 859. (0.0) | 70 | 2p 4p | $^3P_0$ | 2 231 743. (0.2) | 2 235 350. | 2 232 782. (0.1) |
| 22 | 2p 3s | $^3P^o_1$ | 1 709 922. (0.1) | 1 711 250. | 1 711 046. (0.0) | 71 | 2p 4p | $^3P_1$ | 2 233 367. (0.1) | 2 235 350. | 2 234 713. (0.0) |
| 23 | 2p 3s | $^3P^o_2$ | 1 712 655. (0.1) | 1 713 900. | 1 713 727. (0.0) | 72 | 2p 4p | $^3P_2$ | 2 234 238. (0.0) | 2 235 350. | 2 235 180. (0.0) |
| 24 | 2p 3s | $^1P^o_1$ | 1 738 200. (0.3) | 1 743 040. | 1 739 718. (0.2) | 73 | 2p 4d | $^3F^o_2$ | 2 236 868. ( –) | – | 2 238 216. ( –) |
| 25 | 2p 3p | $^1P_1$ | 1 746 573. (0.1) | 1 748 120. | 1 747 844. (0.0) | 74 | 2p 4d | $^3F^o_3$ | 2 238 744. ( –) | – | 2 240 126. ( –) |
| 26 | 2p 3p | $^3D_1$ | 1 754 038. (0.1) | 1 755 470. | 1 755 314. (0.0) | 75 | 2p 4d | $^1D^o_2$ | 2 239 512. (0.1) | 2 241 210. | 2 240 728. (0.0) |
| 27 | 2p 3p | $^3D_2$ | 1 755 312. (0.1) | 1 756 470. | 1 756 575. (0.0) | 76 | 2p 4p | $^1D_2$ | 2 240 645. ( –) | – | 2 241 804. ( –) |
| 28 | 2p 3p | $^3D_3$ | 1 757 821. (0.1) | 1 758 970. | 1 759 043. (0.0) | 77 | 2p 4d | $^3F^o_4$ | 2 240 951. ( –) | – | 2 242 301. ( –) |
| 29 | 2p 3p | $^3S_1$ | 1 769 176. (0.1) | 1 770 380. | 1 770 506. (0.0) | 78 | 2p 4d | $^3D^o_1$ | 2 244 211. (0.2) | 2 248 250. | 2 245 305. (0.1) |
| 30 | 2p 3p | $^3P_0$ | 1 776 847. (0.1) | 1 778 690. | 1 777 823. (0.0) | 79 | 2p 4d | $^3D^o_2$ | 2 244 746. (0.2) | 2 248 250. | 2 245 924. (0.1) |
| 31 | 2p 3p | $^3P_1$ | 1 777 974. (0.0) | 1 778 690. | 1 778 928. (0.0) | 80 | 2p 4f | $^1F_3$ | 2 245 713. ( –) | – | 2 247 165. ( –) |
| 32 | 2p 3p | $^3P_2$ | 1 779 442. (0.0) | 1 779 990. | 1 780 368. (0.0) | 81 | 2p 4d | $^3D^o_3$ | 2 246 210. (0.1) | 2 248 250. | 2 247 192. (0.0) |
| 33 | 2p 3d | $^3F^o_2$ | 1 784 961. ( –) | – | 1 786 049. ( –) | 82 | 2p 4f | $^3F_4$ | 2 246 289. ( –) | – | 2 247 857. ( –) |
| 34 | 2p 3d | $^3F^o_3$ | 1 786 999. ( –) | – | 1 788 095. ( –) | 83 | 2p 4f | $^3F_3$ | 2 246 295. ( –) | – | 2 247 532. ( –) |
| 35 | 2p 3d | $^1D^o_2$ | 1 788 309. (0.1) | 1 789 640. | 1 789 216. (0.0) | 84 | 2p 4f | $^3F_2$ | 2 246 487. ( –) | – | 2 247 527. ( –) |
| 36 | 2p 3d | $^3F^o_4$ | 1 789 052. ( –) | – | 1 790 110. ( –) | 85 | 2p 4p | $^1S_0$ | 2 246 795. ( –) | – | 2 256 277. ( –) |
| 37 | 2p 3p | $^1D_2$ | 1 797 843. (0.1) | 1 795 870. | 1 799 156. (0.2) | 86 | 2p 4d | $^3P^o_2$ | 2 247 691. (0.1) | 2 249 450. | 2 249 335. (0.0) |
| 38 | 2p 3d | $^3D^o_1$ | 1 806 157. (0.1) | 1 807 320. | 1 807 101. (0.0) | 87 | 2p 4d | $^3P^o_1$ | 2 248 163. (0.1) | 2 249 970. | 2 249 955. (0.0) |
| 39 | 2p 3d | $^3D^o_2$ | 1 806 711. (0.1) | 1 807 860. | 1 807 645. (0.0) | 88 | 2p 4d | $^3P^o_0$ | 2 248 402. (0.1) | 2 249 970. | 2 250 287. (0.0) |
| 40 | 2p 3d | $^3D^o_3$ | 1 807 763. (0.1) | 1 808 860. | 1 808 678. (0.0) | 89 | 2p 4f | $^3G_3$ | 2 249 196. ( –) | – | 2 251 070. ( –) |
| 41 | 2p 3d | $^3P^o_2$ | 1 814 627. (0.0) | 1 815 220. | 1 815 554. (0.0) | 90 | 2p 4f | $^3G_4$ | 2 249 537. ( –) | – | 2 251 533. ( –) |
| 42 | 2p 3d | $^3P^o_1$ | 1 815 504. (0.0) | 1 816 210. | 1 816 418. (0.0) | 91 | 2p 4f | $^3G_5$ | 2 250 337. ( –) | – | 2 252 907. ( –) |
| 43 | 2p 3d | $^3P^o_0$ | 1 815 952. (0.0) | 1 816 730. | 1 81 6859. (0.0) | 92 | 2p 4f | $^1G_4$ | 2 251 731. ( –) | – | 2 254 126. ( –) |
| 44 | 2p 3p | $^1S_0$ | 1 829 350. ( –) | – | 1 831 807. ( –) | 93 | 2p 4f | $^3D_3$ | 2 253 098. ( –) | – | 2 254 413. ( –) |
| 45 | 2p 3d | $^1F^o_3$ | 1 837 205. (0.1) | 1 834 690. | 1 839 246. (0.2) | 94 | 2p 4f | $^3D_2$ | 2 253 641. ( –) | – | 2 254 676. ( –) |
| 46 | 2p 3d | $^1P^o_1$ | 1 842 786. (0.1) | 1 841 560. | 1 844 360. (0.2) | 95 | 2p 4f | $^3D_1$ | 2 254 628. ( –) | – | 2 255 643. ( –) |
| 47 | 2s 4s | $^3S_1$ | 2 038 676. ( –) | – | 2 040 211. ( –) | 96 | 2p 4f | $^1D_2$ | 2 255 803. ( –) | – | 2 256 864. ( –) |
| 48 | 2s 4s | $^1S_0$ | 2 048 829. ( –) | – | 2 050 281. ( –) | 97 | 2p 4d | $^1F^o_3$ | 2 256 381. (0.0) | 2 256 570. | 2 259 361. (0.1) |
| 49 | 2s 4p | $^3P^o_0$ | 2 063 614. ( –) | – | 2 064 808. ( –) | 98 | 2p 4d | $^1P^o_1$ | 2 258 053. (0.0) | 2 258 310. | 2 260 557. (0.1) |

**Notes.** Key: $i$: level index; Conf.: configuration; Level: level IC designation; $E_{th}$: theoretical level energy ($cm^{-1}$), this work; $E_{NIST}$: observed energy from the NIST database and reference Martin & Zalubas (1980) ($cm^{-1}$); $E_{CHIANTI}$: previous theoretical calculation by Del Zanna et al. (2008) as in the CHIANTI database; %: percentage difference between theoretical and NIST data.

increases as a factor $z^2$ too, with respect to the background. The relative strength of the background can also increase with increasing charge due to increased spin-orbit mixing, for example, in singlet-triplet mixing. This effect is clearly seen in the transition 1–3. The spin-orbit mixing of $^3$P with $^1$P turns this transition into a dipole-allowed one for iron, with corresponding asymptotic behavior, while in carbon (with a much lower nuclear charge) it behaves as a forbidden transition still.

For the case of $Fe^{22+}$, we show also in Fig. 2 a comparison with the distorted wave results of Bhatia & Mason (1981). While there is good agreement between the distorted wave collision strengths and the background $R$-matrix ones, the omission of resonances by the former method can give rise to significant differences in Maxwellian rate coefficients for some transitions. Chidichimo et al. (1999, 2005) compared their $R$-matrix results for ground-state transitions to levels of $n = 2$ and 3 with

**Table 6.** $Fe^{22+}$ target levels.

| $i$ | Conf. | Level | $E_{th}$ ( %) | $E_{NIST}$ | $E_{CHIANTI}$ ( %) | $i$ | Conf. | Level | $E_{th}$ ( %) | $E_{NIST}$ | $E_{CHIANTI}$ ( %) |
|---|---|---|---|---|---|---|---|---|---|---|---|
| 1 | $2s^2$ | $^1S_0$ | 0. ( –) | 0. | 0. ( –) | 50 | 2s 4p | $^3P^o_1$ | 12 031 666. (0.1) | 12 024 000. | 12 037 753. (0.1) |
| 2 | 2s 2p | $^3P^o_0$ | 348 558. (0.1) | 348 180. | 345 707. (0.7) | 51 | 2s 4p | $^3P^o_2$ | 12 044 813. (0.2) | 12 024 000. | 1 2049 581. (0.2) |
| 3 | 2s 2p | $^3P^o_1$ | 381 443. (0.6) | 379 125. | 377 693. (0.4) | 52 | 2s 4p | $^1P^o_1$ | 12 049 120. (0.0) | 12 044 000. | 12 054 558. (0.1) |
| 4 | 2s 2p | $^3P^o_2$ | 476 579. (1.0) | 471 780. | 469 121. (0.6) | 53 | 2s 4d | $^3D_1$ | 12 082 163. (0.1) | 12 073 000. | 12 087 052. (0.1) |
| 5 | 2s 2p | $^1P^o_1$ | 763 088. (1.4) | 752 410. | 756 439. (0.5) | 54 | 2s 4d | $^3D_2$ | 12 083 884. (0.1) | 12 075 000. | 12 088 720. (0.1) |
| 6 | $2p^2$ | $^3P_0$ | 961 670. (0.6) | 956 100. | 953 971. (0.2) | 55 | 2s 4d | $^3D_3$ | 12 086 965. (0.0) | 12 081 000. | 12 091 694. (0.1) |
| 7 | $2p^2$ | $^3P_1$ | 1 034 199. (0.7) | 1 027 200. | 1 023 195. (0.4) | 56 | 2s 4d | $^1D_2$ | 12 106 784. (0.1) | 12 098 000. | 12 111 606. (0.1) |
| 8 | $2p^2$ | $^3P_2$ | 1 083 341. (1.1) | 1 071 700. | 1 071 669. (0.0) | 57 | 2s 4f | $^3F^o_2$ | 12 110 226. ( –) | – | 12 115 606. ( –) |
| 9 | $2p^2$ | $^1D_2$ | 1 219 566. (1.3) | 1 204 200. | 1 205 136. (0.1) | 58 | 2s 4f | $^3F^o_3$ | 12 111 016. ( –) | – | 12 116 413. ( –) |
| 10 | $2p^2$ | $^1S_0$ | 1 441 242. (1.3) | 1 422 600. | 1 427 089. (0.3) | 59 | 2s 4f | $^3F^o_4$ | 12 112 542. ( –) | – | 12 117 921. ( –) |
| 11 | 2s 3s | $^3S_1$ | 8 913 141. (0.2) | 8 894 000. | 8 919 391. (0.3) | 60 | 2s 4f | $^1F^o_3$ | 12 117 174. ( –) | – | 12 122 994. ( –) |
| 12 | 2s 3s | $^1S_0$ | 8 982 363. ( –) | – | 8 991 141. ( –) | 61 | 2p 4s | $^3P^o_0$ | 12 374 984. ( –) | – | 12 378 557. ( –) |
| 13 | 2s 3p | $^3P^o_0$ | 9 081 428. (0.1) | 9 076 000. | 9 085 799. (0.1) | 62 | 2p 4s | $^3P^o_1$ | 12 379 931. ( –) | – | 12 383 443. ( –) |
| 14 | 2s 3p | $^3P^o_1$ | 9 081 493. (0.1) | 9 076 000. | 9 085 708. (0.1) | 63 | 2p 4p | $^3D_1$ | 12 423 791. (0.2) | 12 443 000. | 12 424 988. (0.1) |
| 15 | 2s 3p | $^1P^o_1$ | 9 112 890. (0.1) | 9 107 000. | 9 116 052. (0.1) | 64 | 2p 4p | $^3P_1$ | 12 450 598. ( –) | – | 12 450 604. ( –) |
| 16 | 2s 3p | $^3P^o_2$ | 9 116 955. (0.5) | 9 076 000. | 9 119 424. (0.5) | 65 | 2p 4p | $^3D_2$ | 12 452 464. (0.1) | 12 443 000. | 12 452 378. (0.1) |
| 17 | 2s 3d | $^3D_1$ | 9 206 351. (0.1) | 9 199 000. | 9 209 350. (0.1) | 66 | 2p 4p | $^3P_0$ | 12 454 533. ( –) | – | 12 455 470. ( –) |
| 18 | 2s 3d | $^3D_2$ | 9 211 353. (0.0) | 9 209 000. | 9 214 241. (0.1) | 67 | 2p 4d | $^3F^o_2$ | 12 475 173. (0.1) | 12 484 000. | 12 475 079. (0.1) |
| 19 | 2s 3d | $^3D_3$ | 9 219 274. (0.1) | 9 212 000. | 9 221 969. (0.1) | 68 | 2p 4d | $^3D^o_2$ | 12 491 404. (0.1) | 12 480 000. | 12 617 081. (1.1) |
| 20 | 2s 3d | $^1D_2$ | 9 282 237. (0.1) | 9 273 000. | 9 286 135. (0.1) | 69 | 2p 4d | $^3F^o_3$ | 12 495 594. (0.1) | 12 484 000. | 12 495 352. (0.1) |
| 21 | 2p 3s | $^3P^o_0$ | 9 355 675. (0.7) | 9 295 000. | 9 358 931. (0.7) | 70 | 2p 4d | $^3D^o_1$ | 12 501 088. (0.1) | 12 488 000. | 12 500 929. (0.1) |
| 22 | 2p 3s | $^3P^o_1$ | 9 373 713. (0.8) | 9 295 000. | 9 376 878. (0.9) | 71 | 2p 4f | $^3G_3$ | 12 506 262. ( –) | – | 12 506 458. ( –) |
| 23 | 2p 3p | $^3D_1$ | 9 467 904. (0.1) | 9 455 000. | 9 467 027. (0.1) | 72 | 2p 4s | $^3P^o_2$ | 12 507 124. ( –) | – | 12 504 270. ( –) |
| 24 | 2p 3s | $^3P^o_2$ | 9 482 883. (2.0) | 9 295 000. | 9 479 551. (2.0) | 73 | 2p 4f | $^3F_2$ | 12 509 812. ( –) | – | 12 509 793. ( –) |
| 25 | 2p 3s | $^1P^o_1$ | 9 530 650. (0.6) | 9 470 000. | 9 527 453. (0.6) | 74 | 2p 4f | $^3F_3$ | 12 510 680. ( –) | – | 12 632 075. ( –) |
| 26 | 2p 3p | $^3D_2$ | 9 534 172. (0.1) | 9 524 000. | 9 532 026. (0.1) | 75 | 2p 4f | $^3G_4$ | 12 510 792. ( –) | – | 12 511 089. ( –) |
| 27 | 2p 3p | $^1P_1$ | 9 535 007. (0.1) | 9 526 000. | 9 533 211. (0.1) | 76 | 2p 4s | $^1P^o_1$ | 12 514 269. ( –) | – | 12 510 866. ( –) |
| 28 | 2p 3p | $^3P_0$ | 9 555 941. (0.9) | 9 644 000. | 9 556 830. (0.9) | 77 | 2p 4p | $^1P_1$ | 12 561 594. ( –) | – | 12 555 470. ( –) |
| 29 | 2p 3d | $^3F^o_2$ | 9 592 492. (0.3) | 9 625 000. | 9 590 854. (0.4) | 78 | 2p 4p | $^3P_2$ | 12 568 548. ( –) | – | 12 587 067. ( –) |
| 30 | 2p 3p | $^3P_1$ | 9 628 099. (0.2) | 9 644 000. | 9 621 590. (0.2) | 79 | 2p 4p | $^3D_3$ | 12 568 748. (0.1) | 12 560 000. | 12 562 210. (0.0) |
| 31 | 2p 3p | $^3D_3$ | 9 635 011. (0.1) | 9 624 000. | 9 627 204. (0.0) | 80 | 2p 4p | $^3S_1$ | 12 573 488. ( –) | – | 12 567 559. ( –) |
| 32 | 2p 3d | $^3F^o_3$ | 9 636 525. (0.1) | 9 625 000. | 9 634 104. (0.1) | 81 | 2p 4p | $^1D_2$ | 12 594 380. ( –) | – | 12 562 508. ( –) |
| 33 | 2p 3d | $^3D^o_2$ | 9 648 575. (0.8) | 9 728 000. | 9 646 734. (0.8) | 82 | 2p 4d | $^3F^o_4$ | 12 608 510. (1.0) | 12 484 000. | 12 601 371. (0.9) |
| 34 | 2p 3p | $^3S_1$ | 9 652 672. ( –) | – | 9 646 155. ( –) | 83 | 2p 4d | $^1D^o_2$ | 12 608 545. (0.1) | 12 597 000. | 12 601 381. (0.0) |
| 35 | 2p 3p | $^3P_2$ | 9 655 675. (0.1) | 9 644 000. | 9 650 043. (0.1) | 84 | 2p 4d | $^3D^o_3$ | 12 616 512. (0.1) | 12 603 000. | 12 609 401. (0.1) |
| 36 | 2p 3d | $^3D^o_1$ | 9 667 523. (0.3) | 9 637 000. | 9 666 720. (0.3) | 85 | 2p 4p | $^1S_0$ | 12 620 702. ( –) | – | 12 615 175. ( –) |
| 37 | 2p 3p | $^1D_2$ | 9 719 656. (0.1) | 9 709 000. | 9 712 806. (0.0) | 86 | 2p 4d | $^3P^o_1$ | 12 624 101. (0.1) | 12 615 000. | 12 617 092. (0.0) |
| 38 | 2p 3d | $^3F^o_4$ | 9 730 703. (1.1) | 9 625 000. | 9 721 889. (1.0) | 87 | 2p 4d | $^3P^o_2$ | 12 624 218. (0.1) | 12 614 000. | 12 490 641. (1.0) |
| 39 | 2p 3d | $^1D^o_2$ | 9 739 968. (1.1) | 9 638 000. | 9 732 187. (1.0) | 88 | 2p 4d | $^3P^o_0$ | 12 625 070. (0.1) | 12 615 000. | 12 618 160. (0.0) |
| 40 | 2p 3d | $^3D^o_3$ | 9 765 214. (0.2) | 9 749 000. | 9 757 889. (0.1) | 89 | 2p 4f | $^1F_3$ | 12 631 755. ( –) | – | 12 624 793. ( –) |
| 41 | 2p 3d | $^3P^o_2$ | 9 784 901. (0.3) | 9 753 000. | 9 777 147. (0.2) | 90 | 2p 4f | $^3F_4$ | 12 634 423. ( –) | – | 12 627 518. ( –) |
| 42 | 2p 3d | $^3P^o_1$ | 9 785 499. (0.3) | 9 753 000. | 9 777 827. (0.3) | 91 | 2p 4f | $^3D_2$ | 12 638 357. ( –) | – | 12 642 692. ( –) |
| 43 | 2p 3d | $^3P^o_0$ | 9 787 882. (0.4) | 9 753 000. | 9 780 122. (0.3) | 92 | 2p 4f | $^3D_3$ | 12 639 026. ( –) | – | 12 510 611. ( –) |
| 44 | 2p 3p | $^1S_0$ | 9 798 347. ( –) | – | 9 792 651. ( –) | 93 | 2p 4f | $^3G_5$ | 12 640 044. ( –) | – | 12 633 552. ( –) |
| 45 | 2p 3d | $^1F^o_3$ | 9 845 559. (0.2) | 9 830 000. | 9 840 612. (0.1) | 94 | 2p 4f | $^1G_4$ | 12 642 268. ( –) | – | 12 636 011. ( –) |
| 46 | 2p 3d | $^1P^o_1$ | 9 855 746. (0.3) | 9 828 000. | 9 850 236. (0.2) | 95 | 2p 4d | $^1F^o_3$ | 12 643 513. (0.1) | 12 631 000. | 12 637 211. (0.0) |
| 47 | 2s 4s | $^3S_1$ | 11 963 752. ( –) | – | 11 973 125. ( –) | 96 | 2p 4f | $^3D_1$ | 12 645 135. ( –) | – | 12 638 337. ( –) |
| 48 | 2s 4s | $^1S_0$ | 11 987 901. (0.1) | 11 981 000. | 11 996 229. (0.1) | 97 | 2p 4d | $^1P^o_1$ | 12 648 318. ( –) | – | 12 641 922. ( –) |
| 49 | 2s 4p | $^3P^o_0$ | 12 029 994. (0.0) | 12 024 000. | 12 036 048. (0.1) | 98 | 2p 4f | $^1D_2$ | 12 649 343. ( –) | – | 12 631 491. ( –) |

**Notes.** Key: $i$: level index; Conf.: configuration; Level: level IC designation; $E_{th}$: theoretical level energy ($cm^{-1}$), this work; $E_{NIST}$: observed energy from the NIST database and reference Sugar & Corliss (1985) ($cm^{-1}$); $E_{CHIANTI}$: previous theoretical calculation by Chidichimo et al. (2005) as in the CHIANTI database; %: percentage difference between theoretical and NIST data.

the distorted wave ones of Bhatia & Mason (1981) and found differences of up to a factor of two and ~30%, respectively, at $10^7$ K.

Figure 3 shows our Maxwell integrated effective collision strengths for the same transitions as shown in Fig. 2. The figure also shows a comparison with the previous benchmark calculations: Berrington et al. (1985); Del Zanna et al. (2008); Chidichimo et al. (2005); Mitnik et al. (2003). The Mitnik et al. (2003) calculation included Laguerre pseudostates in the close-coupling expansion. It was performed in *LS*-coupling and a direct comparison without further recoupling can only be made for transitions which involve a singlet state (or an S-state), following a generalization of Burgess et al. (1970), Eq. (99) etc. For the singlet–triplet transitions, level resolution can be determined simply by multiplying the effective collision strength by the fractional statistical weight of the level. The inclusion of pseudostates gives a difference of less than 10% compared to calculations without them.

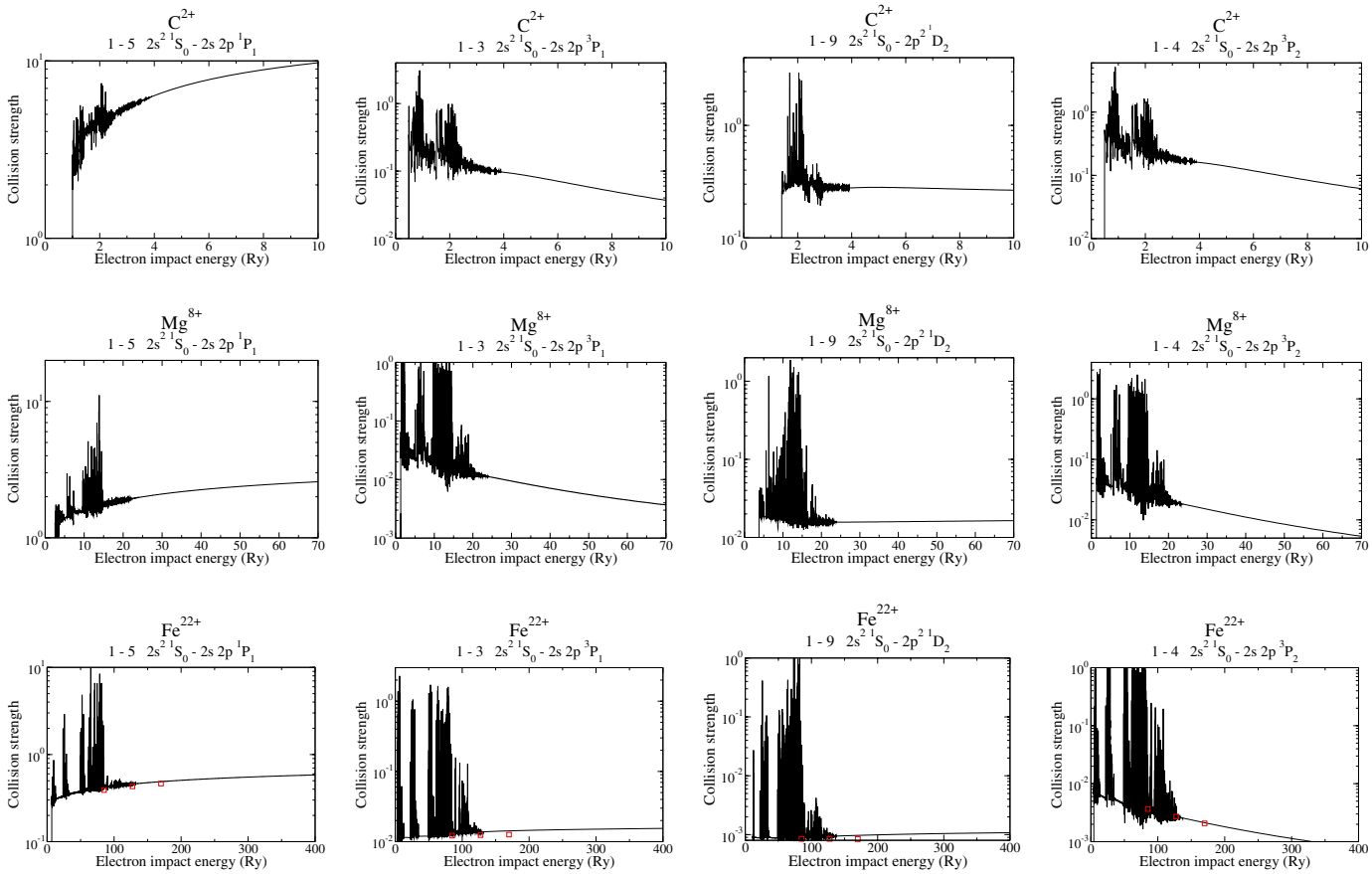


**Fig. 2.** Electron-impact excitation collision strengths versus the impact energy for some selected transitions within the $n = 2$ complex for the benchmark ions. Full line: present $R$-matrix work; □: distorted wave results of Bhatia & Mason (1981).

For low temperatures, the center of the Maxwellian envelope lies on the resonance region, so such temperatures are quite sensitive to the good description of the resonances, if the impact energy mesh is fine enough. Thus, we have carried out a convergence study of the effective collision strengths at low temperature and we have checked that the fine mesh step used is sufficient for the ions under consideration. Overall, excellent agreement with previous calculations is found. This indicates that resonance excitation due to the extra configurations in our extended target does not produce significant enhancements for the $n = 2$ transitions. The transition (1−3) shows when the spin orbit gives an important contribution. For carbon and magnesium this transition behaves as forbidden for temperatures of physical interest, but for iron it shows dipole behavior.

The main population mechanism to states which radiate the important lines for plasma diagnosis (electric dipole $2p^2-2s2p$) is direct excitation from the ground state. A secondary population mechanism lies in the direct excitation from the ground state to $n = 3$ and $n = 4$ levels and afterwards cascade to these $2p^2$ levels. The most intense transitions to $n = 3$ calculated in the present work mainly agree with previous $R$-matrix calculations and also with the interpolated data, but some discrepancies were found in weaker transitions, double electron jumps or forbidden ones.

Effective collision strengths for weak transitions can have a considerable contribution from resonances at lower temperatures. The present close-coupling expansion is larger than those used in previous (non-pseudo-state) $R$-matrix works, especially those which only expanded up to $n = 3$. Consequently, we expect a larger resonance enhancement compared to those works, and we illustrate a case in Fig. 4. There we compare our effective collision strengths for the $2s^2\ ^1S_0-2s3p\ ^3P_1$ transition in $Ne^{6+}$ with the $LS$-plus-algebraic recoupling $R$-matrix results of Ramsbottom et al. (1995). At low temperatures our results display a much larger resonance enhancement, compared to those of Ramsbottom et al. (1995), while at high temperatures we see the influence of spin-orbit mixing turning the high-energy/temperature tail from a forbidden to weak dipole-allowed one.

Figure 5 shows the effective collision strengths for some selected transitions of $P^{11+}$. Be-like $P^{11+}$ has not been calculated before using the $R$-matrix method or a DW method, and the data currently used for diagnostic modeling within the CHIANTI database are interpolated ones from Keenan (1988). In this figure we show the same set of transitions as in Fig. 3. The double-electron-jump (1−9) shows differences between the $R$-matrix calculations and the interpolated data, and in the spin-changing transition (1 − 3) the discrepancy is quite large. Asymptotically, the transition 1−3 behaves as a dipole one through spin-orbit mixing, as discussed earlier. But, algebraic recoupling only of $LS$-coupling data does not include such mixing and it (1−3) behaves as a forbidden one still. Thus, neither the original data nor the interpolated data are valid for such transitions, at these energies.

We close this section with a note of caution: we have shown only a selection of transitions and when the totality of excitations plus-cascade are modeled then Del Zanna et al. (2008) has shown that significant problems can arise on using interpolated data.

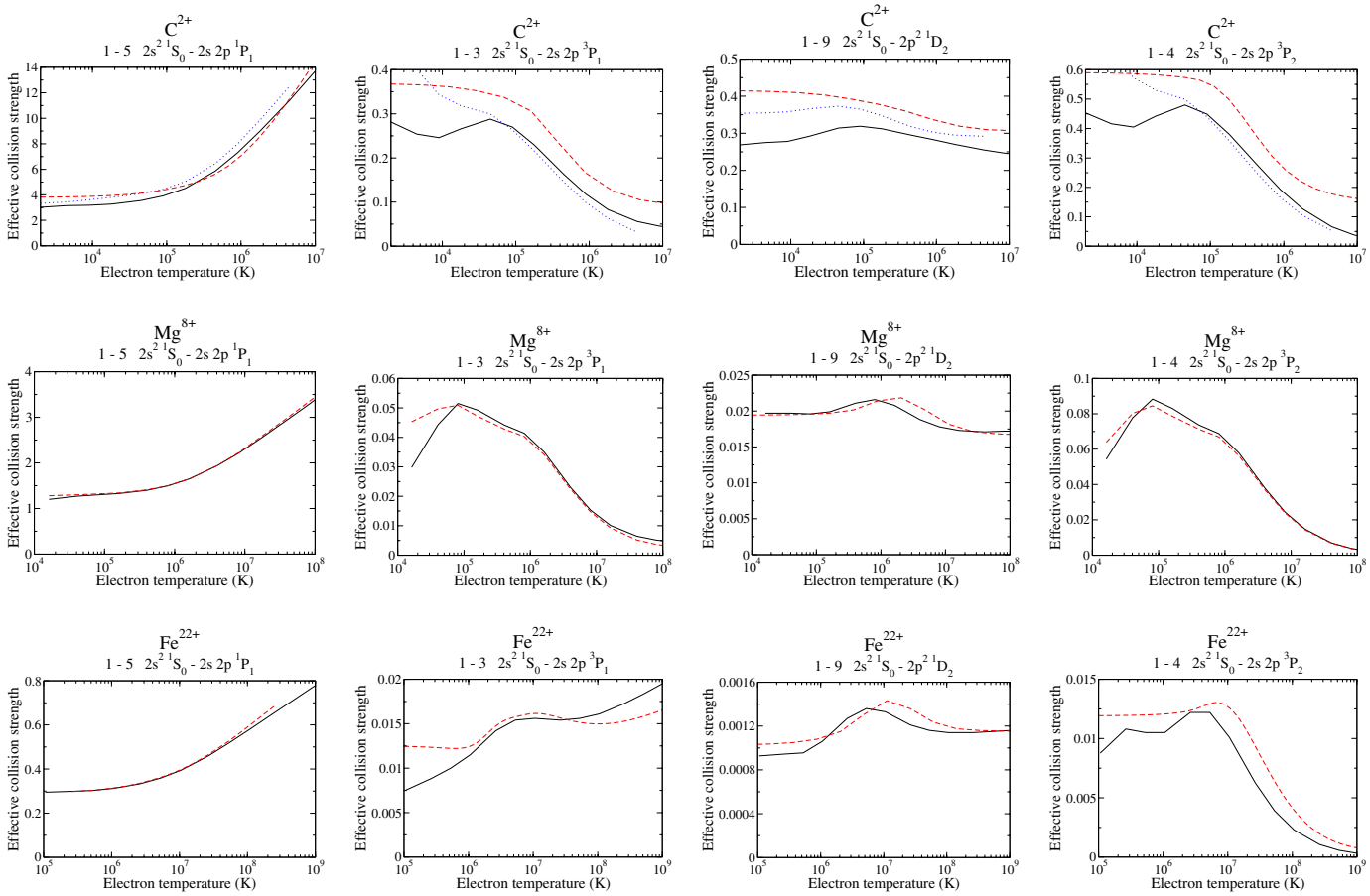


**Fig. 3.** Electron-impact excitation effective collision strengths versus the electron temperature for some selected transitions and targets, as in Fig. 2. Full line: present work; dashed line: $C^{2+}$ Berrington et al. (1989), $Mg^{8+}$ Del Zanna et al. (2008), and $Fe^{22+}$ Chidichimo et al. (2005); dotted line: $C^{2+}$ Mitnik et al. (2003).

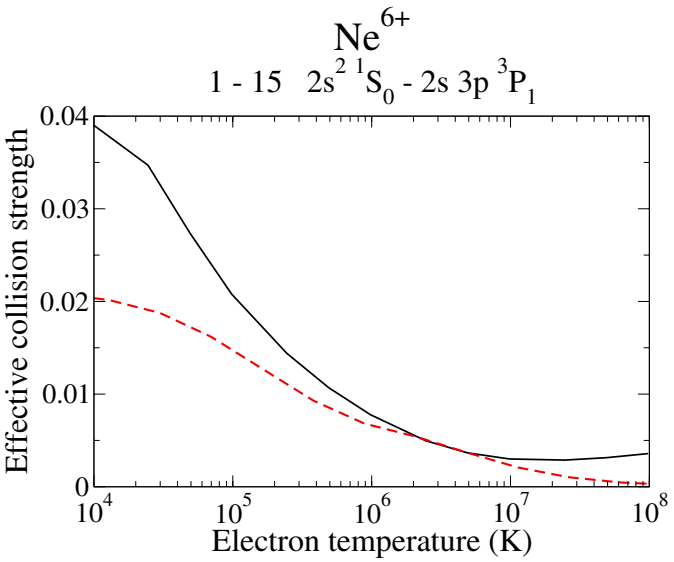


**Fig. 4.** Electron-impact excitation effective collision strengths versus the electron temperature for transition 1−15 $2s^2\,{}^1S_0-2s3p\,{}^3P_1$ of $Ne^{6+}$. Full line: present work; dashed line: Data from Ramsbottom et al. (1995).

## 5. Conclusions

We have presented a complete data set of ICFT *R*-Matrix calculations of electron-impact excitation of all ions in the Be-like isoelectronic sequence from $B^+$ to $Zn^{26+}$. We have shown a selected set of collision strengths and effective collision strengths for some important $n = 2$ transitions and ions, finding good agreement with previous similar calculations. The present work expands the previous ones Del Zanna et al. (2008); Chidichimo et al. (2003, 2005) for Be-like Mg, Fe and Ni, by significantly increasing the orbitals in the basis set.

The present data set constitutes a significant improvement over previous available data for many ions in the Be-like sequence, which was based upon interpolated data. With our basis set emission lines including from cascade effects from levels up to $n = 7$ can be predicted. With the present data, emission lines from Be-like ions can reliably be used for diagnostics of temperature and density of astrophysical and fusion plasmas. The atomic data are made available at our APAP network web page[2]. They will also be uploaded into the OPEN-ADAS[3] and CHIANTI[4] databases.

Work is in progress to expand the method to other isoelectronic sequences, in particular, the Mg-like, which is similar to this one in the sense that it consist of a closed *n*-shell plus two electrons.

*Acknowledgements.* The present work was funded by STFC (UK) through the University of Strathclyde UK APAP network grant ST/J000892/1 and the University of Cambridge DAMTP astrophysics grant.

[2] http://www.apap-network.org
[3] http://open.adas.ac.uk
[4] http://www.chiantidatabase.org

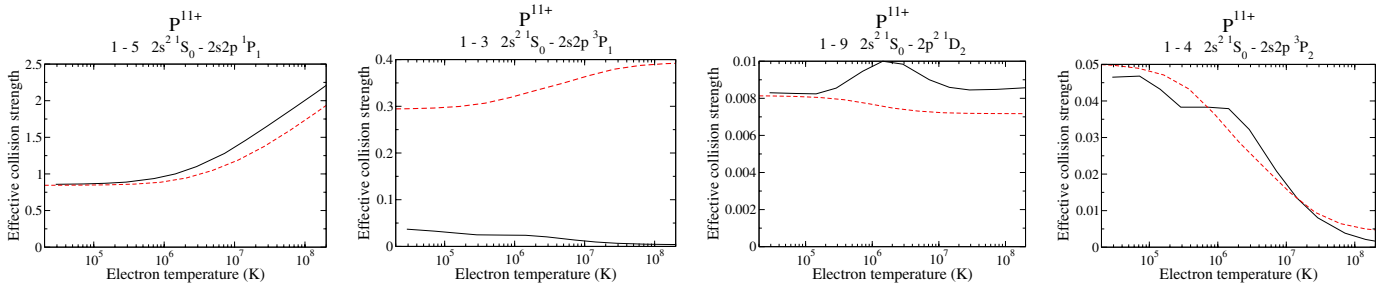


**Fig. 5.** Electron-impact excitation effective collision strengths versus the electron temperature for some selected transitions of $P^{11+}$. Full line: present work; dashed line: interpolated data from Keenan (1988).

## References


Audard, M. 2003, Adv. Space Res., 32, 927
Badnell, N. R. 2011, Comput. Phys. Commun., 182, 1528
Badnell, N. R., & Griffin, D. C. 1999, J. Phys. B, 32, 2267
Badnell, N. R., & Griffin, D. C. 2001, J. Phys. B, 34, 681
Badnell, N. R., Griffin, D. C., & Mitnik, D. M. 2003, J. Phys. B At., Mol. Opt. Phys., 36, 1337
Berrington, K. A., Burke, P. G., Dufton, P. L., & Kingston, A. E. 1985, Atom. Data Nucl. Data Tables, 33, 195
Berrington, K. A., Burke, V. M., Burke, P. G., & Scialla, S. 1989, J. Phys. B, Atomic, Molecular and Optical Physics, 22, 665
Berrington, K. A., Eissner, W. B., & Norrington, P. H. 1995, Comput. Phys. Commun., 92, 290
Bhatia, A. K., & Landi, E. 2007, Atom. Data Nucl. Data Tables, 93, 275
Bhatia, A. K., & Mason, H. E. 1981, A&A, 103, 324
Burgess, A. 1974, J. Phys. B, At. Mol. Phys., 7, L364
Burgess, A., & Tully, J. A. 1992, A&A, 254, 436
Burgess, A., Hummer, D. G., & Tully, J. A. 1970, Philos. Trans. R. Soc. London, Ser. A, 266, 225
Burgess, A., Chidichimo, M. C., & Tully, J. A. 1997, J. Phys. B, 30, 33
Chidichimo, M. C., Zeman, V., Tully, J. A., & Berrington, K. A. 1999, A&AS, 137, 175
Chidichimo, M. C., Badnell, N. R., & Tully, J. A. 2003, A&A, 401, 1177
Chidichimo, M. C., Del Zanna, G., Mason, H. E., et al. 2005, A&A, 430, 331
Del Zanna, G., & Mason, H. E. 2005, A&A, 432, 1137
Del Zanna, G., Rozum, I., & Badnell, N. R. 2008, A&A, 487, 1203
Dere, K. P. 1978, ApJ, 221, 1062
Dere, K. P., Landi, E., Mason, H. E., Monsignori-Fossi, B. C., & Young, P. R. 1997, A&AS, 125, 149
Dufton, P. L., Kingston, A. E., & Scott, N. S. 1983, J. Phys. B., 16, 3053
Eissner, W. M., Jones, M., & H, N. 1974, Comput. Phys. Commun., 8, 270
Griffin, D. C., Badnell, N. R., & Pindzola, M. S. 1998, J. Phys. B, 31, 3713
Hummer, D. G., Berrington, K. A., Eissner, W., et al. 1993, A&A, 279, 298
Inoue, T., Nakai, M., Tanaka, A., et al. 2001, Plasma Phys. Control. Fusion, 43, L9
Keenan, F. P. 1988, Phys. Scr., 37, 57
Keenan, F. P., Berrington, K. A., Burke, P. G., Dufton, P. L., & Kingston, A. E. 1986, Phys. Scr., 34, 216
Li, F., Liang, G. Y., Bari, M. A., & Zhao, G. 2013, A&A, 556, A32
Liang, G. Y., Badnell, N. R., & Zhao, G. 2012, A&A, 547, A87
Martin, W. C. & Zalubas, R. 1980, J. Phys. Chem. Ref. Data, 9, 1
Mitnik, D. M., Griffin, D. C., Ballance, C. P., & Badnell, N. R. 2003, J. Phys. B, At. Mol. Opt. Phys., 36, 717
Moore, C. E. 1993, in Tables of Spectra of Hydrogen, Carbon, Nitrogen and Oxygen Atoms and Ions, ed. J. W. Gallacher, CRC Series in Evaluated Data in Atomic Physics (CRC Press)
Neupert, W. M., Gates, W., Swartz, M., & Young, R. 1967, ApJ, 149, L79
Ramsbottom, C. A., Berrington, K. A., & Bell, K. L. 1994a, J. Phys. B, 27, L811
Ramsbottom, C. A., Berrington, K. A., Hibbert, A., & Bell, K. L. 1994b, Phys. Scr., 50, 246
Ramsbottom, C. A., Berrington, K. A., & Bell, K. L. 1995, Atom. Data Nucl. Data Tables, 61, 105
Sampson, D. H., Goett, S. J., & Clark, R. E. H. 1984, Atom. Data Nucl. Data Tables, 30, 125
Sandlin, G. D., Bartoe, J.-D. F., Tousey, R., & Van Hoosier, M. E. 1986, ApJS, 61, 801
Sugar, J., & Corliss, C. 1985, J. Phys. Chem. Ref. Data, 14, Suppl. 2, 1
Summers, H. P., Dickson, W. J., Boileau, A., et al. 1992, Plasma Physics and Controlled Fusion, 34, 325
Tachiev, G., & Fischer, C. F. 1999, J. Phys. B, 32, 5805
Vernazza, J. E., & Reeves, E. M. 1978, ApJS, 37, 485
Wilhelm, K., Marsch, E., Dwivedi, B. N., et al. 1998, ApJ, 500, 1023
Witthoeft, M. C., Whiteford, A. D., & Badnell, N. R. 2007, J. Phys. B, At. Mol. Opt. Phys., 40, 2969
Zhang, H. L., & Sampson, D. H. 1992, Atom. Data Nucl. Data Tables, 52, 143